National Aeronautics and Space Administration

3D X-ray CT for BGA/CGA Workmanship Defect Detection

Reza Ghaffarian, Ph.D.
Jet Propulsion Laboratory
Pasadena, California

Jet Propulsion Laboratory
California Institute of Technology
Pasadena, California

JPL Publication 12-21 12/12

National Aeronautics and Space Administration

3D X-ray CT for BGA/CGA Workmanship Defect Detection

NASA Electronic Parts and Packaging (NEPP) Program
Office of Safety and Mission Assurance

Reza Ghaffarian, Ph.D.
Jet Propulsion Laboratory
Pasadena, California

NASA WBS: 724297.40.43
JPL Project Number: 104593
Task Number: 40.49.02.08

Jet Propulsion Laboratory
4800 Oak Grove Drive
Pasadena, CA 91109

http://nepp.nasa.gov

This research was carried out at the Jet Propulsion Laboratory, California Institute of Technology, and was sponsored by the National Aeronautics and Space Administration Electronic Parts and Packaging (NEPP) Program.

Acknowledgments

The author would like to acknowledge many people from industry and the Jet Propulsion Laboratory (JPL) who were critical to the progress of this activity. The author extends his appreciation to program managers of the National Aeronautics and Space Administration Electronics Parts and Packaging (NEPP) Program, including Michael Sampson, Ken LaBel, Dr. Charles Barnes, and Dr. Douglas Sheldon, for their continuous support and encouragement.

Objectives and Products

Commercial-off-the-shelf (COTS) advanced microelectronic technologies in high-reliability versions are now being considered for use in a number of National Aeronautics and Space Administration (NASA) electronic systems. One of the key drawbacks of advanced electronic packages with hidden solder joint interconnections, such as the column grid array (CGA), is that inspection can be challenging—whether visually or using X-rays. In general, inspection for solder joint integrity is poor, except for identifying shorts. The new, advanced X-ray systems, especially the 3D computer tomography version, may be able to provide the three-dimensional features that are extremely difficult to resolve under the 2D systems.

This report presents both 2D and 3D X-ray images along with their representative optical photomicrographs for a number of advanced electronics package assemblies. The 2D X-ray inspection data for 3D stack and CGA package assemblies are presented. Key features detectable by a 2D X-ray system show the limitation of this inspection tool. The 3D computer tomography X-ray system has the added capability of combining 360-degree slices of single images into a 3D volumetric image. Static images of slices from 3D X-ray were compared to 2D X-ray images. The key advantage and disadvantage of each X-ray system were presented based on the comparison of images taken for each system.

Given NASA's emphasis on the workmanship of microelectronic packages and assemblies, understanding key features of various inspection systems that detect defects in the early stages of assembly is critical to developing approaches that will minimize future failures. Additional specific, tailored non-destructive inspection approaches could enable low-risk insertion of these advanced electronic packages.

Key words: Real time X-ray, two-dimensional X-ray, three-dimensional X-ray, 2D X-ray, 3D X-ray, Column grid array, stack package, CGA, 3D stack, solder joint reliability, thermal cycle

TABLE OF CONTENTS

1.0 EXECUTIVE SUMMARY

X-ray transmission radiography is an inspection technique in which x radiation passes through a specimen to produce a shadow image of its internal structure. X-ray radiography, in its static film version, was for decades a common nondestructive evaluation technique for electronics parts and hybrid electronics. For example, MIL-STD-883 once defined the X-ray feature requirements for small-scale electronic devices. Real-time X-ray detection systems, which replaced film radiography, are now widely used to define features and select areas of interest for further evaluation. With the advancement of microelectronics with much smaller feature sizes, real-time X-ray has now become a necessity for inspecting and detecting fine and hidden features of electronic packages and assemblies. Magnifications of 1000X are now obtainable from commercially available equipment.

Figure 1-1 compares visual and X-ray inspection approaches for defect detection, especially for solder joint interconnections. X-ray is specifically useful for features such as package internal wire bond anomalies, assembly solder joint voids, bridges, missing elements, and geometric changes in feature sizes. In other cases, visual inspection is far superior to X-ray detection for solder joint defects, including dewetting, microcracks, and cold and disturb anomalies. It is therefore critical to evaluate the limitations of various types of X-ray systems for detecting damage and cracking and inspecting hidden solder joints. Ideally, a combination of various inspection techniques may need to be performed in order to assure quality at part, package, and system levels.

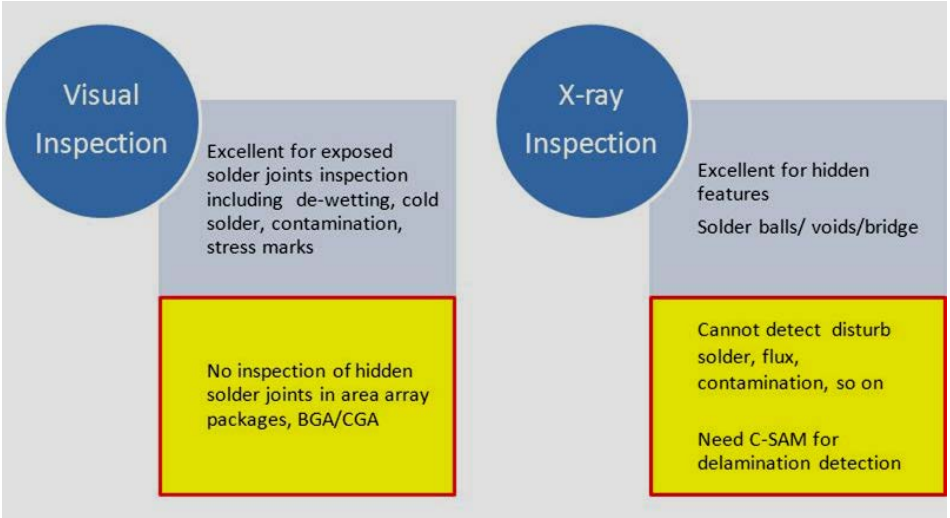

Figure 1-1. Strengths and weaknesses of using X-ray vs. visual inspection to detect key solder joint defects.

This reports presents evaluations performed using 2D X-ray with its enhanced sample rotation and software (3D tomography), as shown in Figure 1-2. The image detector's rotational feature allows better definition of package and assembly by concentrating X-rays onto specific features and avoiding blockage by other elements. This added feature also allows X-ray images to be gathered by rotating the sample and then combining the images to allow cross-sectional viewing of package and assembly. The volume covered by sample rotation limits the closeness of both X-ray and detector, therefore limiting the magnification of 3D features compared to than 2D X-ray versions.

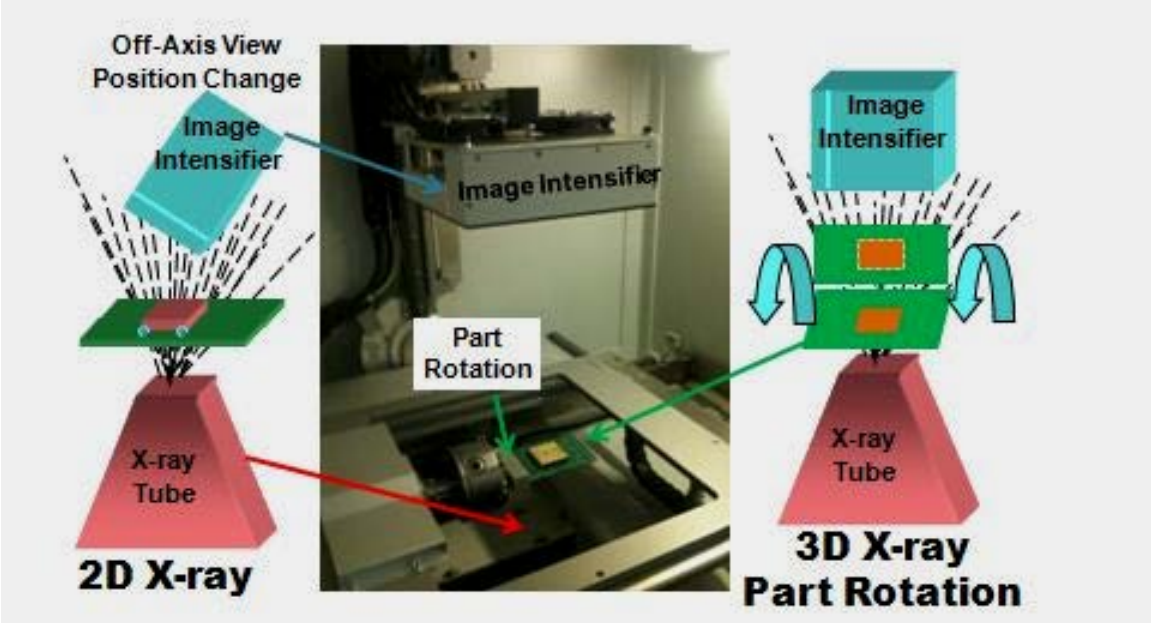

Figure 1-2. Features of 2D and 3D X-ray tomography with a photo of the X-ray system used in this investigation.

The report presents both 2D and 3D X-ray images, along with their representative optical photomicrographs, for a number of advanced electronics package assemblies. Key images gathered and compared are:

- 2D and 3D X-ray images for a thermally cycled 3D TSOP stack package were gathered and compared to their optical images. Optical images clearly showed solder joint cracks and lift, but 2D or 3D X-ray did not.
- 2D and 3D X-ray images were gathered for a number of column grid array (CGA) package assemblies after thermal cycling. Optical inspections showed crack and damage to the outer rows of columns. Note that CGAs are integrated circuit packages with solder column underneath the package; solder joints are formed with these columns under the package.

Given NASA's emphasis on the workmanship of microelectronic packages and assemblies, understanding key features of various inspection systems that detect defects in the early stages of assembly is critical to developing approaches that will minimize future failures. Additional specific, tailored non-destructive inspection approaches could enable low-risk insertion of these advanced electronic packages.

2.0 X-RAY TECHNOLOGY

2.1 X-Ray Definition and Use for Advanced Electronics

Even though X-ray was discovered more than a century ago, its practical applications were limited due to the lack of readily available magnification and imaging technologies. Increased inspection demands for package and assembly applications—quality controls needed for the aerospace and automotive industries in particular—further helped technological development of X-ray. It is only within the last few decades that X-ray inspection has evolved from industrial imaging to microfocus and nanofocus, with various detection approaches. X-rays systems now enable detection of hidden defects not detectable by optical microscopes or machine vision systems. Microfocus and nanofocus enable inspectors to detectthe finer electronic features of advanced electronics packages and assemblies.

X-rays are high-energy electromagnetic radiation with shorter wavelengths than ultraviolet light, but longer wavelengths than gamma rays. They are invisible and highly penetrable depending on the X-ray's energy, which increases with frequency. As frequency and thus penetration increase, the type of X-ray moves from "soft" to "hard." For high reliability electronic applications, visual inspection is traditionally performed by quality assurance personnel at various package and assembly build steps, especially for solder joint interconnections. However, visual inspection are not adequate for ensuring the integrity of advanced electronic packages and assemblies, such as CGAs and 3D stack technologies with hidden solder joints—2D and 3D X-ray systems may be used to alleviate some of these inspection limitations.

2.2 X-Ray for Ensuring CGA/3D Stack Package/Assembly Integrity

Previous generations of microelectronic packaging technology aimed mostly at meeting the needs of high-reliability applications, such as the ceramic leaded quad flat package (CQFP). Visual inspection was adequate for ensuring the quality of CQFP solder joint integrity. Consumer electronics now driving miniaturization trends for electronic packaging and assembly introduce a vast number of area array packages with hidden solder joints and other challenges to the inspectability for solder joint integrity. Most current package types are transitioning to Pb-free solder alloy in order to enforcing restrictions on hazardous substances (ROHS) for electronic systems. The solder joint appearance for the new materials is not shiny, which will add confusion to visual inspection of Pb-free solders in high-reliability applications.

Until recently, high-reliability applications have successfully utilized ceramic versions of plastic packages, such as the plastic ball-grid-array (PBGA) or its analogous ceramic ball-grid-array (and column-grid-array; CBGA and CGA). Today, there are fewer ceramic versions and they are generally lagging in technology compared to plastic ones [1-6]. X-ray inspection is used for ensuring the quality of area array packages and assemblies and detecting levels of voids and bridges of solder joints hidden under packages. Ceramic substrates are heavier and less penetrable to X-ray radiation than plastic, making them even more difficult to inspect for defects under ceramic area array package assemblies. More penetrable X-ray power is needed. X-ray tools are needed that can achieve the power needed to penetrate and image the parts, as well as the resolution to examine details. Historically, an increase in power results in a loss of resolution, such that lower resolution and higher power X-ray sources are unable to sufficiently inspect the assembly while fully intact. Recent technological improvements in X-ray target materials have narrowed the gap between power requirements and resolution needs.

The 3D version of these packages are either purely stacks of area array packages or other complex versions, and each layer is less visible to 2D X-ray systems because of the complex interaction of image layers in the stacks. Only 3D X-ray systems may be able to separate layers and enable better defect detection of solder joints and other package/assembly anomalies.

2.3 Visual and X-Ray Inspection Comparison

For high-reliability electronic applications, traditionally, quality assurance personnel are responsible to performs visual inspection at various package and assembly build steps. For example, at assembly level, solder joints are inspected and either accepted or rejected based on specific sets of workmanship requirements. Further assurance of electronic subsystems or systems is gained by subsequent short-time environmental exposures, including thermal cycles, vibration, and mechanical shock testing. These screening tests also allow progress of workmanship anomalies and failures due to workmanship defects or design flaws at either subsystem or system levels. For space applications, visual inspection alone is generally performed at the prepackage stage, prior to its closure (pre-cap), as well as at several steps during assembly and at subsystem levels.

For both leaded and leadless package solder joints, the author has performed visual inspections at different magnifications to correlate damage rankings due to thermal cycling exposures to those revealed by cross-sectioning [7, 8]. An example of such correlation is shown in Figure 2.3-1. Numerous leaded and leadless package assemblies were subjected to thermal cycling, removed at intervals, inspected visually and by scanning electron microscopy (SEM). Results were then correlated to cross-sectioning images. Generally, good correlations were found between ranking the levels of crack formation by visual inspection projection and subsequently by cross-sectional evaluation.

Visual inspection and advanced optical microscopy, while very effective for standard electronics, may have limited usefulness for extremely small, dense electronics. It also provides some usefulness for area array packages, but no value for hidden ball/column arrays under the package. SEM and other advanced magnification tools may be used for inspection of miniature packages, but generally are not suitable for assembly systems because of size limitations. Even for packages, sample size and potential damage due electrostatic discharge (ESD) during SEM evaluation limits the wider usages of such advanced evaluation techniques.

The inspection system’s ability to identify, measure, and analyze defect data after assembly is also critical. Inspection of the solder joint integrity of BGAs/CGAs is important, but cannot be effectively performed by visual inspection. Inspection of fine internal structures of microelectronics assemblies and the alignment of hidden microcircuit interconnect structures, bridges, and voids in BGA/CGA assemblies, may be carried out using real-time X-ray techniques. Internal package delamination, however, cannot be detected by X-ray; other tools, such as cross-sectional acoustic microscopy (C-SAM), are needed for such evaluation.

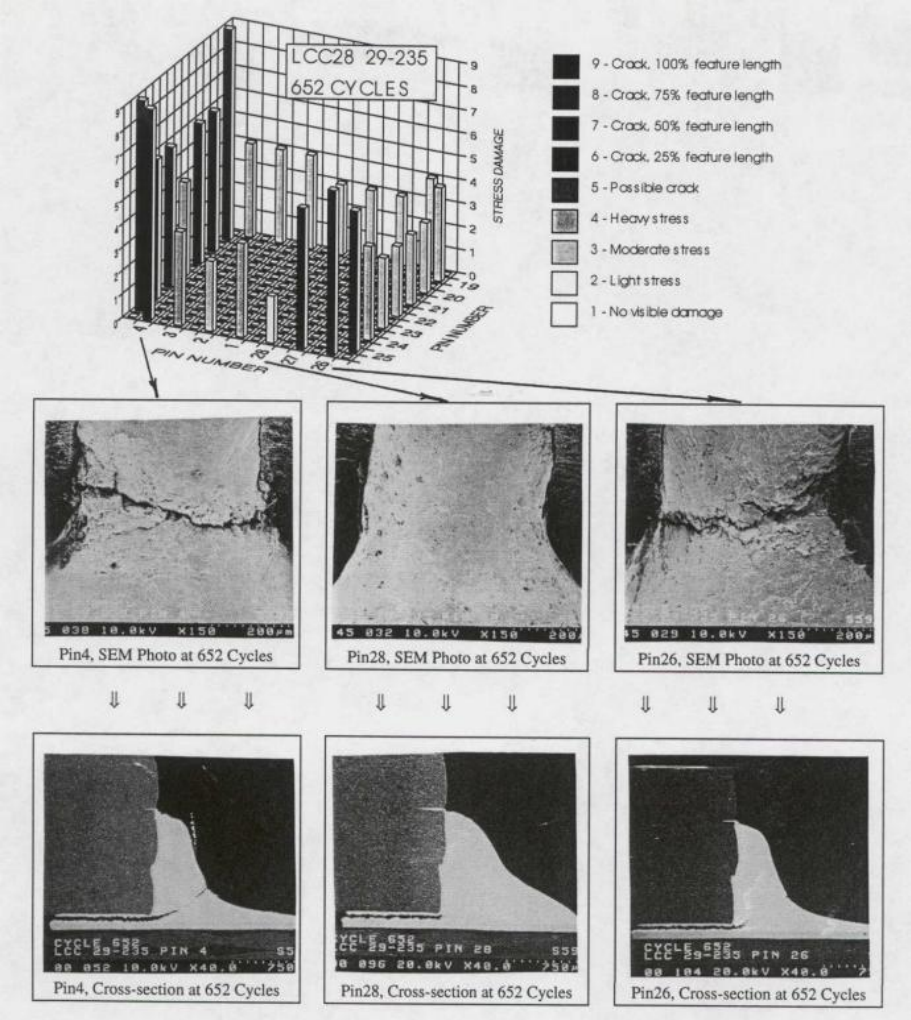

Figure 2.3-1. Comparison of qualitative projection by visual inspection and verification by X-sectioning for ceramic leadless package assembly [7,8].

In summary, X-ray inspection is excellent for detecting hidden features such as voids as well as geometric measurements. Visual inspection, however, can better detect solder joint workmanship defects such as de-wetting, crack, cold solder, and disturb solders. Table 2.3-1 summarizes the key advantages of each technique, which are:

- X-ray is excellent for detecting porosity and voids in solder and geometric measurement of solder thickness and volume.
- Visual inspection is excellent for detecting stress marks, cracks, open contacts, cold and disturb solder joints, dull solder, and flux residue and contamination.
- X-ray and visual inspection both clearly can detect exposed solder balls and bridge. However, only X-ray can detect hidden defects or other features.

For this reason, this investigation was performed to evaluate limitation of 2D/2D X-ray systems for detecting damage/cracking and hidden solder joints. Ideally, a combination of various inspection techniques is required for ensuring quality of advanced microelectronics at package and system levels.

Table 2.3-1. Key solder joint defect types and the ability to detect them by X-ray or visually, using an optical microscope.

Visible Features	X-Ray Inspection	Visual Inspection
Stress marks, Cracks	0	+++
Open Contacts	0	++
Cold/Disturb Joint	0	+++
Dull Solder	0	+++
Flux Residue/Contamination	0	+++
Porosity and Voids in Solder	+++	0
Solder Thickness/Volume	+++	0
Heel/Toe Side Fillets	+++	++
Solder Balls	+++	++
Solder Bridge	+++	++

+++ Excellent detection
++ Good detection
0 Poor or unacceptable

2.4 2D Real Time X-Ray

The transmission X-ray captures everything between the X-ray source and image intensifier, since X-rays are emitted from the source and travel through the sample. The higher the density of the sample, e.g., heavy ceramic package and columns in CGAs, the fewer X-rays will pass through and be captured by the image intensifier. The captured X-rays are displayed in a grayscale image, with the lower density areas, such as voids, appearing brighter than the higher density, darker areas. The voltage and current of the X-ray's intensity can be adjusted to reveal features of the sample sections of greatest interest.

Real-time 2D X-ray systems typically have an X-ray source, an image detector, and a sample holder. Figure 2.4-1 shows features of four types of 2D X-ray systems. One type is a standard X-ray inspection system with a microfocus source and a stationary image intensifier as the detector. The other type is also a 2D X-ray tool with a similar microfocus source intensity and stationary position, but the detector has off-axis rotational capability.

The standard top-down X-ray system with a stationary detector is limited to 2D inspections and small sample rotation/tilt. The sample holder can be used to manually hold a sample in a desired oblique angle to better define selected features. This is a cumbersome and time-consuming approach.

The top-down 2D X-ray systems are very effective in testing single-sided assemblies. With the use of a sample manipulator, an oblique view angle enhances inspection of both single- and double-sided assemblies, with some loss of magnification due to increase in distance between source and detector. Experience is needed in discerning between bottom-side board elements and actual solder and component defects. This can be very difficult or even impossible on extremely dense assemblies. In any case, only certain solder-related defects such as voids, misalignments, solder shorts, etc., are easily identified by transmission systems. However, even an experienced operator can miss other anomalies such as insufficient solder, apparent open connections, and cold solder joints.

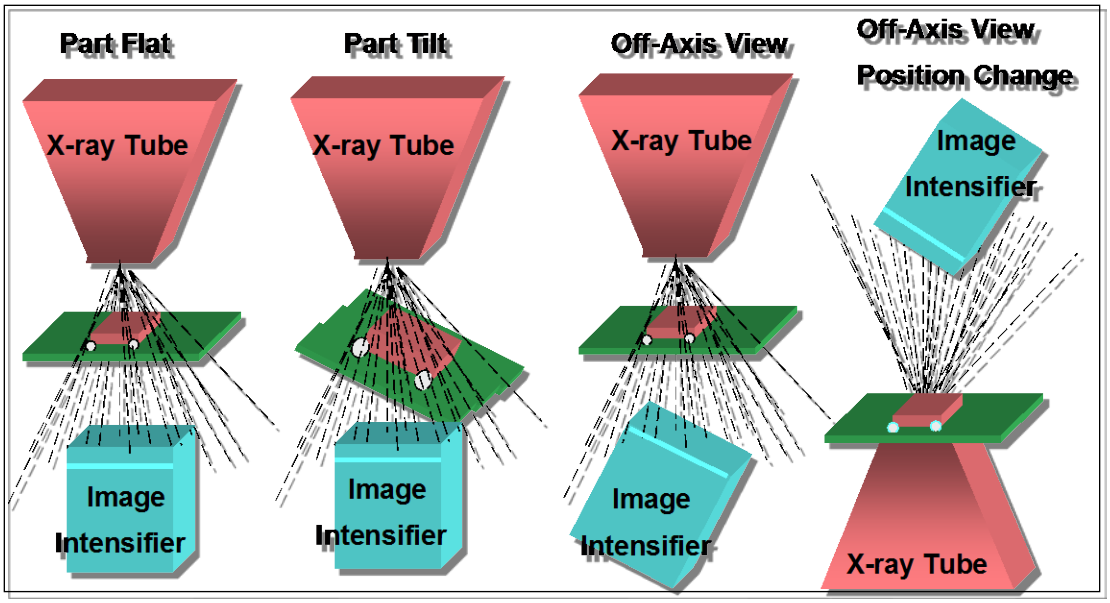

Figure 2.4-1. Various 2D X-ray systems with stationary and rotational parts and image intensifiers.

2.5 3D Computed Tomography (CT) X-Ray

A real-time 2D X-ray system with an X-ray source and image detector is expanded to computer tomography (CT) when software capability is added to capture a large number of X-ray images, with storing and retrieving, as specified (see Figure 2.5-1). X-ray tubes typically generate either fan beams or cone beams depending on the type of detector. In the Feldkamp method [9], a 3D CT system with cone-processing digital geometry, the 3D image is generated from the inside of an object from a large series of 2D images of a single-axis of rotation. In the 3D X-ray, several layers are created per rotation, each layer similar to that of a 2D X-ray, with the X-ray source positioned across from the detector and the sample between the two sources for scanning.

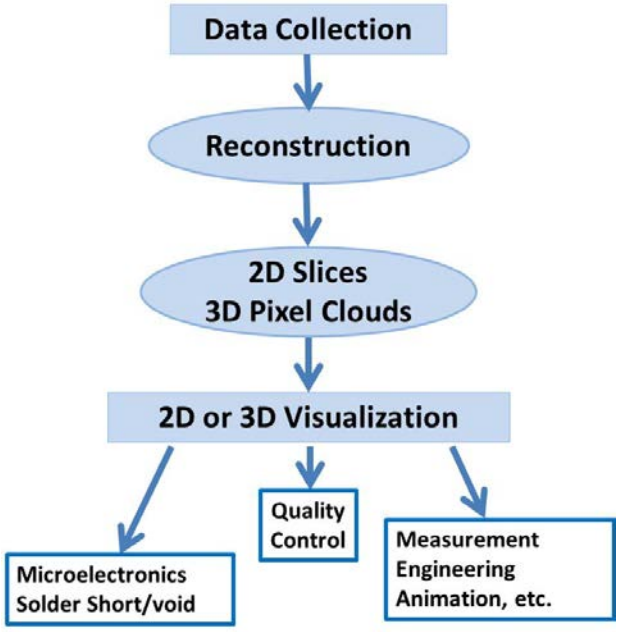

Figure 2.5-1. Flow diagram of 3D X-ray reconstruction from 2D X-ray slices.

Figure 2.5-2 illustrates the Feldkamp method of 2D-to-3D image transformation. The CT image is created by capturing a digital format; a series of X-ray images with the relative positional coordinates of each image that is captured. These data are captured and stored while the object is rotated within the X-ray beam. When all of the digital data have been captured, the data bank is processed to reconstruct the cross-sectional 2D or 3D images. The processing is carried out using powerful software (in this case Windows-based) specifically developed for CT. When performing a CT scan, the scan creates what are called sinograms. A sinogram is a matrix of projections that represents one attenuation of the beam. Each line in the sinogram represents a separate angle. Sinogram CT also creates what are called tomograms. Tomogram is a virtual slice of the test piece where black represents the air. When creating a CT scan, there is a transformation between pixels and voxels. A pixel is a picture element in two dimensions, whereas a voxel is a volume element in three dimensions. Each pixel now represents the new volume block and the volume displayed by the accumulated layers.

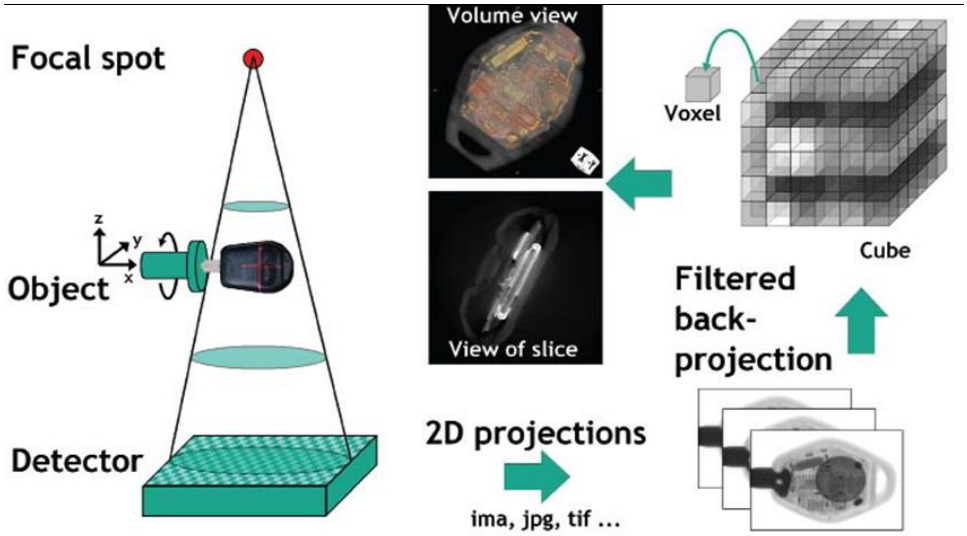

Figure 2.5-2. Cone beam reconstruction for the microfocus 3D µCT X-ray inspection (Feldkamp method [9]).

Configuration and specifications of this X-ray system are:

- Geometric magnification up to 2,800 x, total magnification up to 10,000 x
- Inspection area of 310 mm × 310 mm (12” × 12”), maximum sample size of 550 mm × 440 mm (21” × 17”)
- Detail detectability down to <500 nm
- 16-bit real-time image processing as standard
- Oblique viewing (140°) at high magnification
- Microfocus computed tomography (µCT)
- High-accuracy µCT sample rotation

3.0 X-RAY TEST RESULTS FOR CGA ASSEMBLIES

3.1 2D X-Ray of CGA Assemblies

Figure 3.1-1 shows X-ray photomicrographs of an assembled ceramic column grid array with 560 columns after thermal cycling, using a 2D X-ray system with an oblique view capability. X-ray images from two views are included. CGA columns having high lead composition (10Sn/90Pb) are much darker than the eutectic solder (63Sn/37Pb) used for attachment to the board. Within lighter solder joints, at lower sections of columns, other lines, possibly caused by cracking, are apparent. Lack of smoothness of patterns may be an indication of solder graininess. This generally occurs due to solder grain growth as thermal cycling progresses.

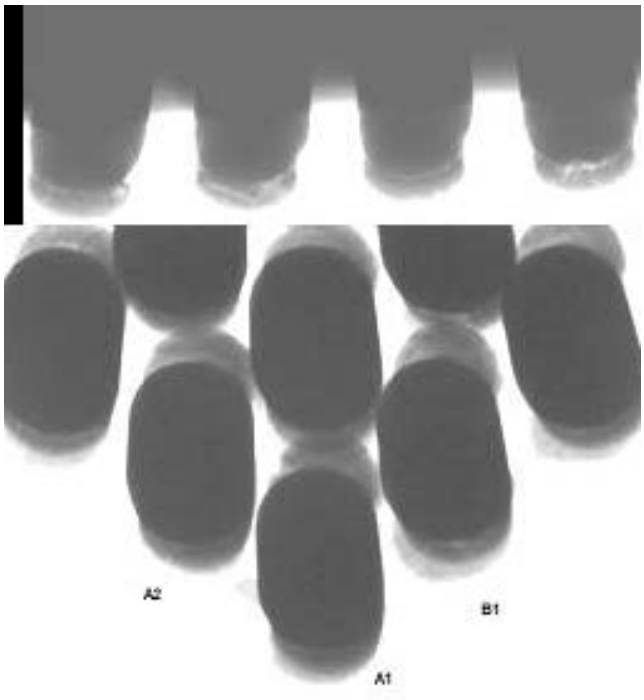

Figure 3.1-1. X-ray photomicrographs of CGA using a 2D X-ray system with a rotational detector at two angles. Signs of cracking/damage are somewhat apparent.

Figures 3.1-2 and 3.1-3 show X-ray features of two CGA 717 I/O assemblies after thermal cycling, one with a non-solder mask defined (NSMD) and the other with a solder mask defined (SMD) pad configuration. To better compare the two pad configurations, the corner solder columns are magnified by bringing the X-ray source close to the top of the packages. No apparent significant differences between the two pad designs are discernible from the 2D X-ray images. The level of damage cannot be discerned by the 2D X-ray system.

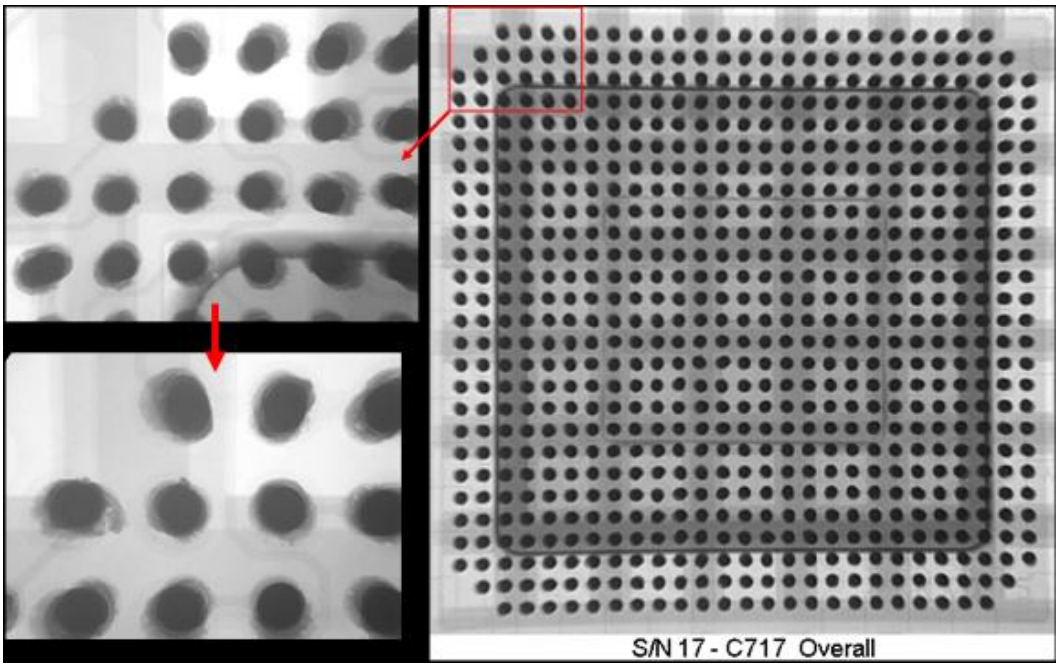

Figure 3.1-2. X-ray photographs of CGA 717 I/O assembly with NSMD pad design after thermal cycling.

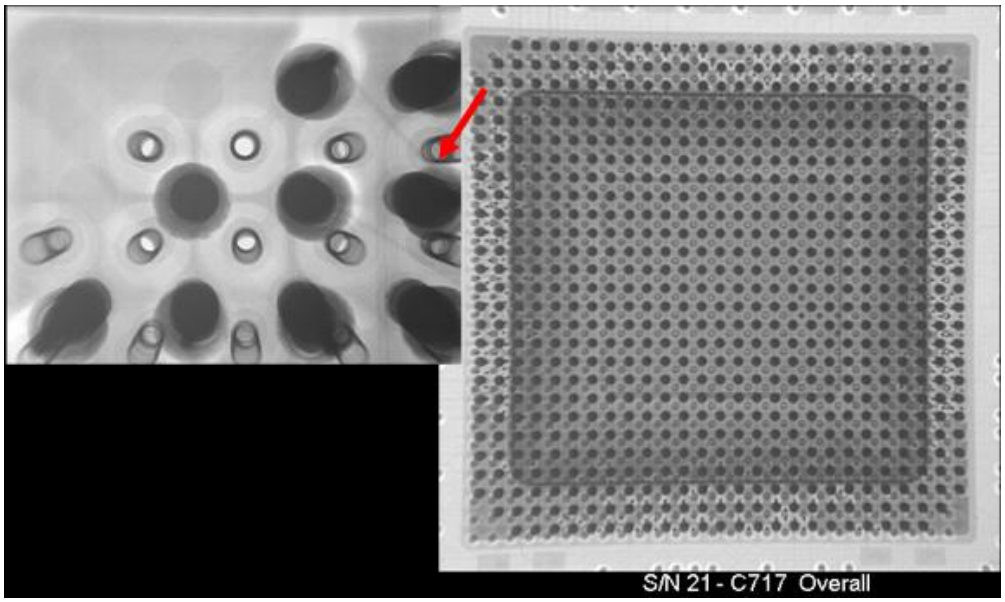

Figure 3.1-3. X-ray photographs of CGA 717 I/O assembly with SMD pad design after thermal cycling.

Figure 3.1-4 shows 2D X-ray images of an assembly CGA with 1144 columns after exposure to thermal cycling. Images of corner solder columns at much higher magnifications are also included in the figure. Figure 3.1-5 compares X-ray images of corner columns for the standard condition when the board is sitting flat (top left) or tilted at an angle (top right). No further improvement was observed in better detecting damage caused by interference of other columns, even with the detector tilting.

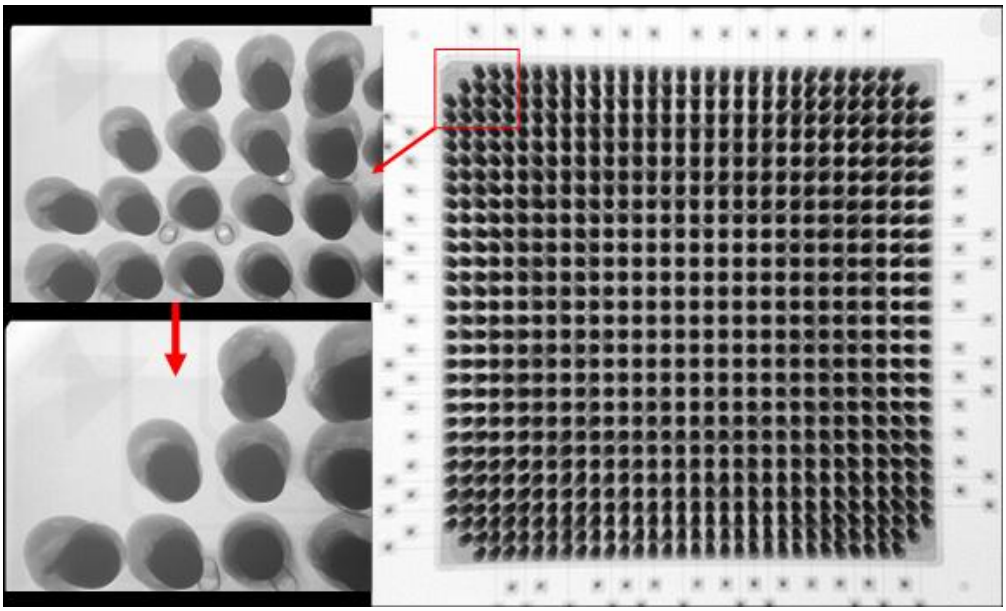

Figure 3.1-4. X-ray photographs of a high I/O CGA assembly after thermal cycling.

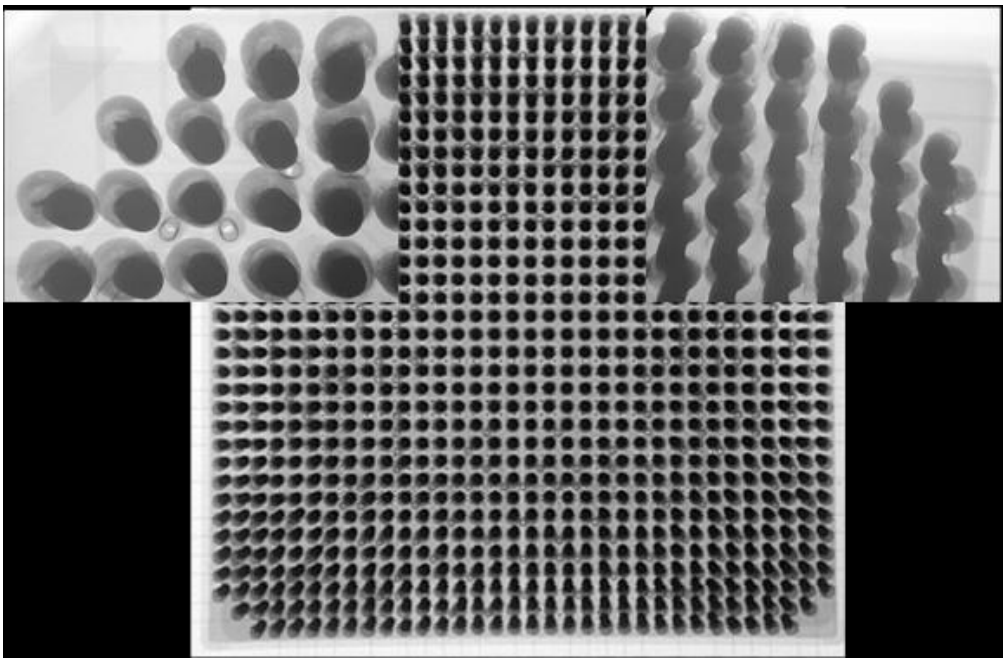

Figure 3.1-5. X-ray photographs of a high I/O CGA assembly showing higher magnification images when the board is sitting flat (top left photo) or tilted at an angle (top right) during X-ray evaluation.

3.2 Optical and 2D/3D X-Ray Characterization of CGA1752 After TC

For comparison purposes, both optical and 2D/3D X-ray images were taken of an assembly CGA with 1752 columns after exposure to thermal cycling. An optical image of this package assembly after a number of thermal cycles is shown in Figure 3.2-1. It clearly shows deformation of solder joints; therefore slight to severe tilt of columns due to thermal cycling and coefficient of thermal expansion (CTE) mismatches of package and printed circuit board. The solder microstructural changes and tilting of columns are more severe for the corner than for center columns, as expected.

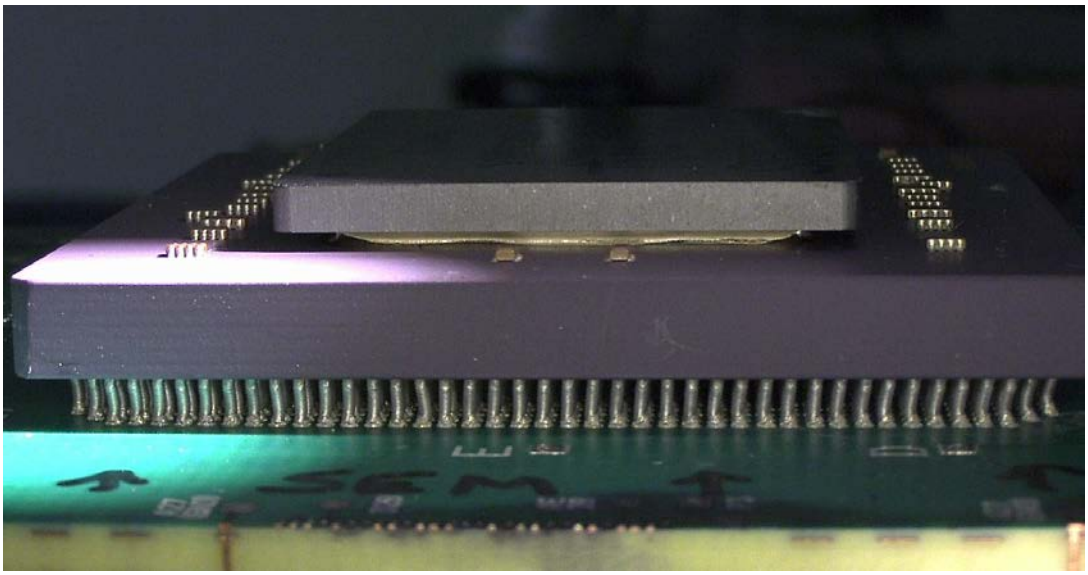

Figure 3.2-1. Optical photograph of a CGA1752 package assembly after thermal cycling.

A few representative 2D X-ray images for this package assembly are shown in Figure 3.2-2. On the top left X-ray image, die and slightly larger heat sink than die are clearly apparent at the center of the package. Around the perimeter, spotted darker areas represent chip capacitors mounted on the package ceramic substrate that are also visually apparent, a specific feature of this high I/O non-hermetic CGA package. The two bottom photos were taken at an angle and higher magnification. Dark cylindrical features are columns and lighter areas at the ends are solder joints. Two shades of lightness are apparent, the lightest areas showing possible separation, while less light areas show solder joint materials with some shift, and this is the case based on visual inspection and optical photomicrographs.

Therefore, the change in X-ray intensity also shows potential damages, especially the shift at the interface between column and solder. Microcracks observed by optical microscopy are not as apparent and it is extremely difficult to determine if indeed lighter appearance is due to microcracks or not (i.e., if there was no prior knowledge of the condition of the CGA assembly). Attempts to better define column damage toward the internal section of the package was impossible because of interference with the X-rays due to heat sink, die, and the ceramic substrate. The low detectability of CGA internal columns is one of the drawbacks of X-ray for CGA packages. Heavy ceramic packaging materials reduce X-ray intensity and interfere with resolution of columns and solder joints under X-ray inspection.

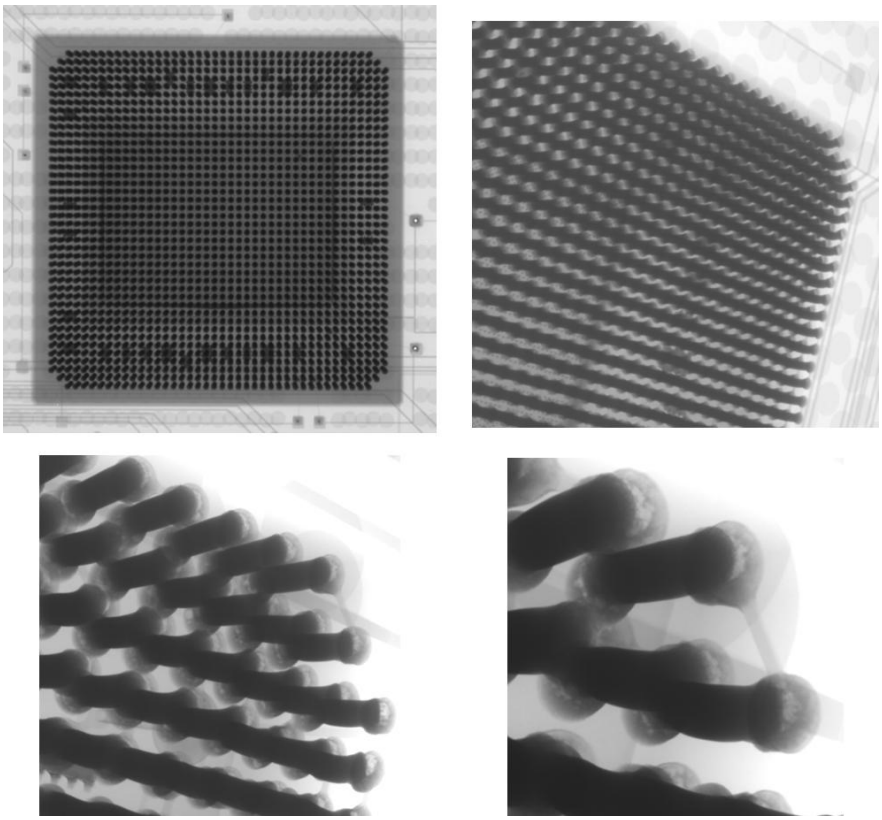

Figure 3.2-2. 2D X-ray photographs of a CGA1752 assembly after thermal cycling.

The X-ray system using the Feldkamp method of 2D-to-3D image conversion was used to characterize thermal cycling damage to a CGA1752 package assembly. The CT images are automatically created by designing a sample holder for insertion into the rotational motor tool installed in the 2D X-ray system. For 3D image gathering, an assembled CGA board was cut no closer than about one-half of an inch away from the part to avoid damaging the part. Ideally, the part to be X-rayed should be as close as possible to the X-ray source in order to achieve higher magnification.

Figure 3.2-3 shows a representative setup to prepare for generating 3D X-ray images. Rotation of the sample allows a series of X-ray images with relative positional coordinates of each image to be captured. These data are stored while the object is rotated within the X-ray beam. When all digital data have been captured, the data bank is processed to reconstruct the cross-sectional 2D or 3D images. Figure 3.2-4 shows a number of X-ray X-sectional images, both horizontal and vertical, taken from the 3D volumetric images. It clearly identifies a few feature of this specific package—decoupling capacitors are apparent when the horizontal image is constructed. Oversize heat sink, die, and overall column features are also apparent.

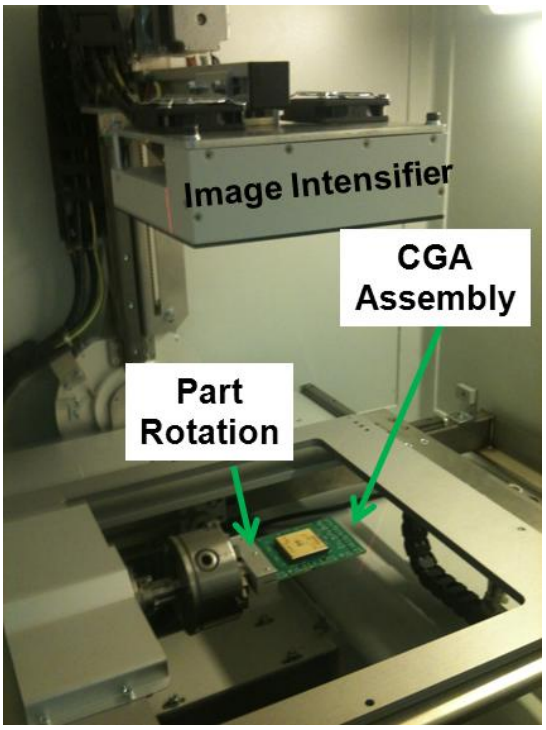

Figure 3.2-3. Photograph of CGA assembly in position and ready for rotation to generate 3D X-ray images.

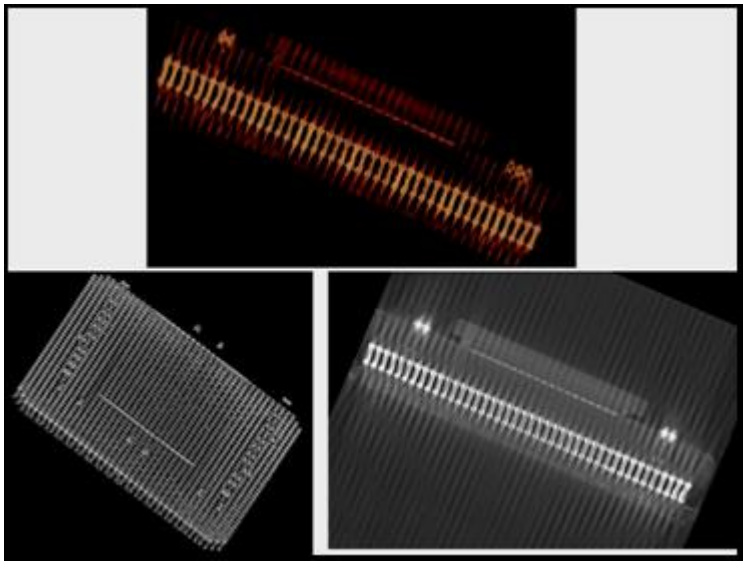

Figure 3.2-4. Slices from 3D X-ray digital data generated by X-section, either vertical or horizontal.

Figure 3.2-5 shows a representative X-ray X-section of a CGA1752 photograph (left side) and the location where such X-sectioning was performed (right side). Column tilting and some signs of damage are apparent, but because of the much lower magnification than with the 2D X-ray images, the exact level of damage could not be clearly identified. Figure 3.2-6 shows an attempt to increase magnification and possibly better delineate damage features. Lower magnification of the 3D images did not allow better identification of damage due to thermal cycling. Improvement was seen when the board was cut close to the package.

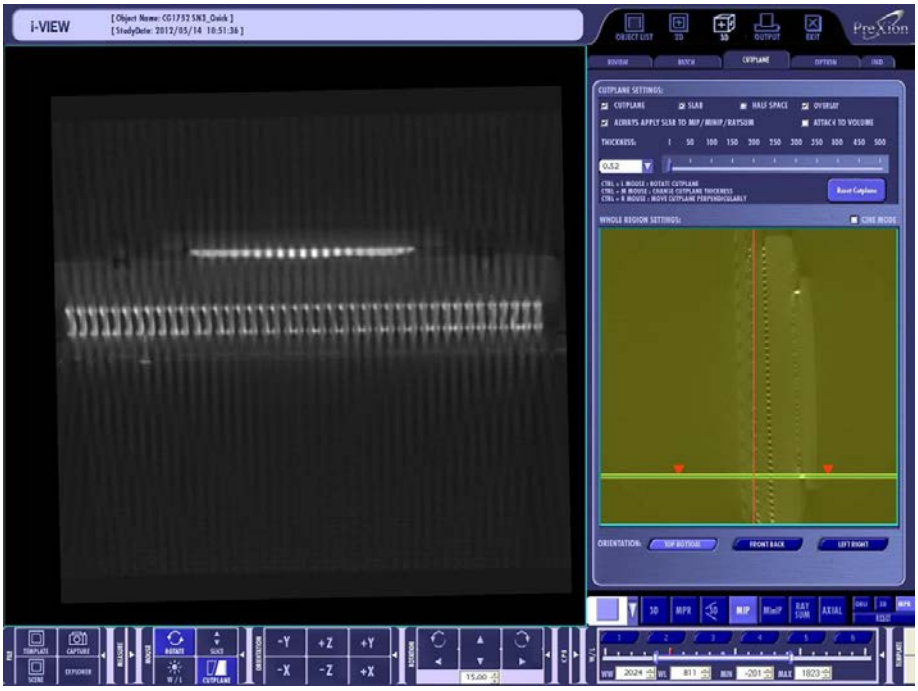

Figure 3.2-5. 3D X-ray photographs of a CGA1752 assembly after thermal cycling.

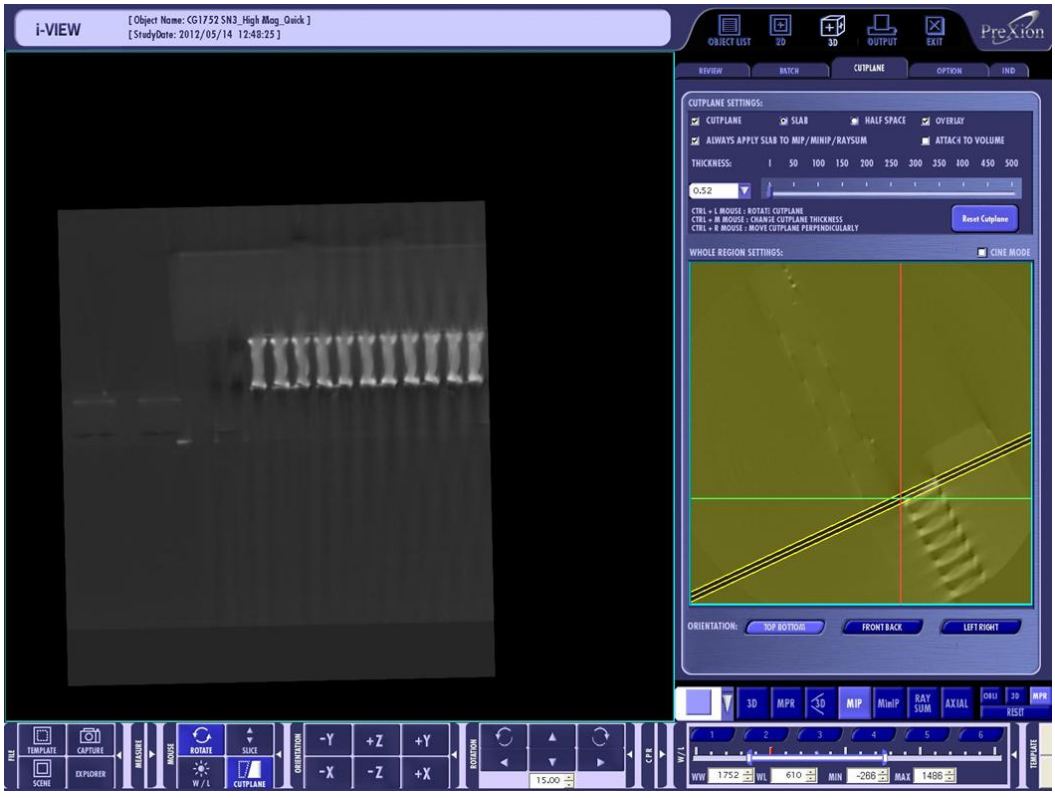

Figure 3.2-6. Higher magnification of 3D X-ray photographs of a CGA1752 assembly.

Figure 3.2-7 shows a few representative 2D X-ray images for another CGA package assembly with 1272 spiral columns that differ from the high-lead columns in CGA1752. On the top left X-ray image, die is clearly apparent at the center of the package. The corner columns are missing and clearly apparent. The two bottom images were taken at an angle and at higher magnification. Less column tilt is apparent compared to the CGA1752 assembly. Dark cylindrical features are columns, and even darker spotted areas represents the copper spiral surrounding the tin-lead solder column. The lighter images at the ends of columns are solder joints engulfing even brighter spherical images. These bright volumes are possibly voids formed at the interface of column and PCB. This needs to be verified through optical microsectioning.

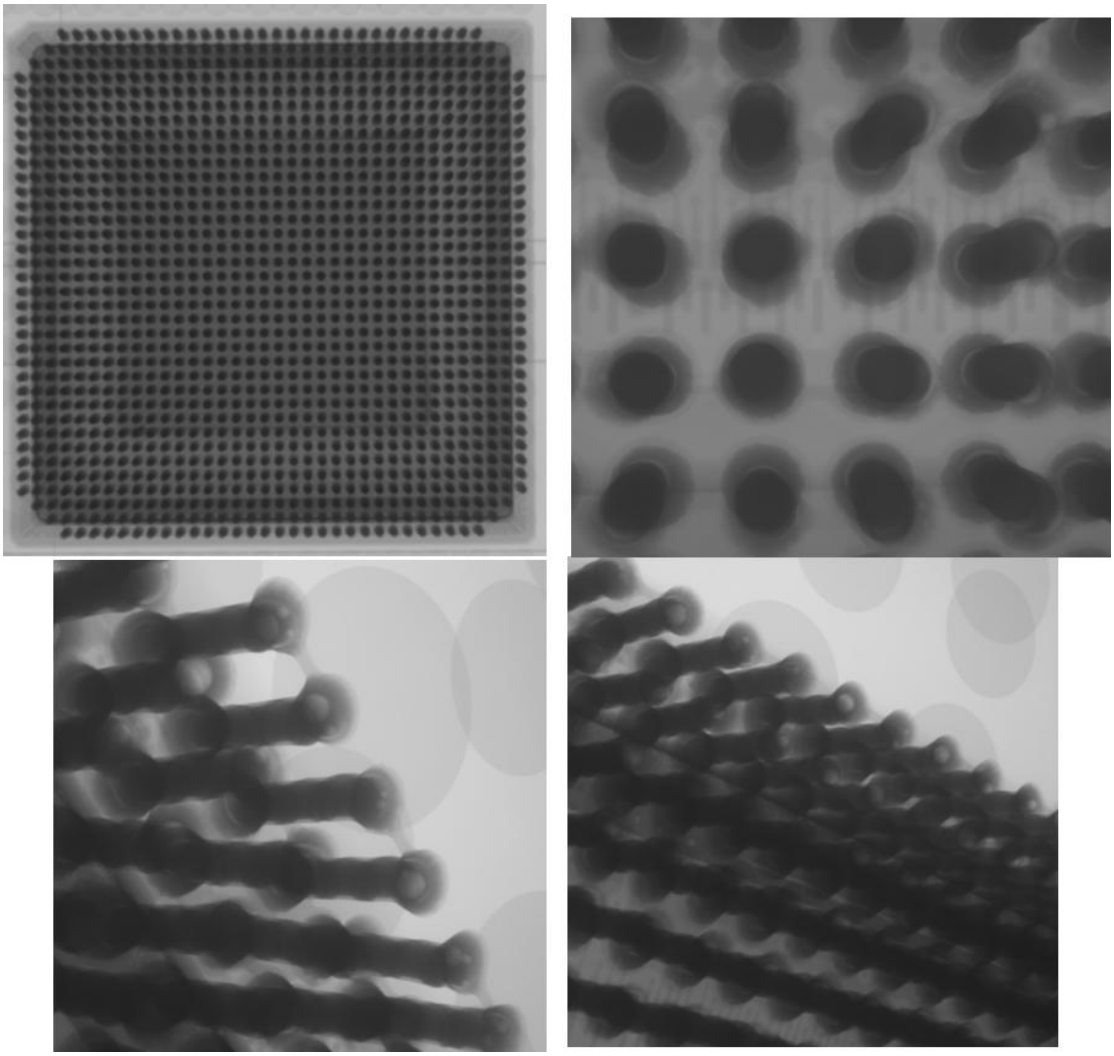

Figure 3.2-7. 2D X-ray photographs of a CGA1272 assembly after thermal cycling.

Figure 3.2-8 shows two representative X-sectional views, vertical and horizontal, from the 3D X-ray tomography of a CGA1272 package assembly after thermal cycling. These columns appear to have tilted and shifted less compared to those for the CGA1752 assembly.

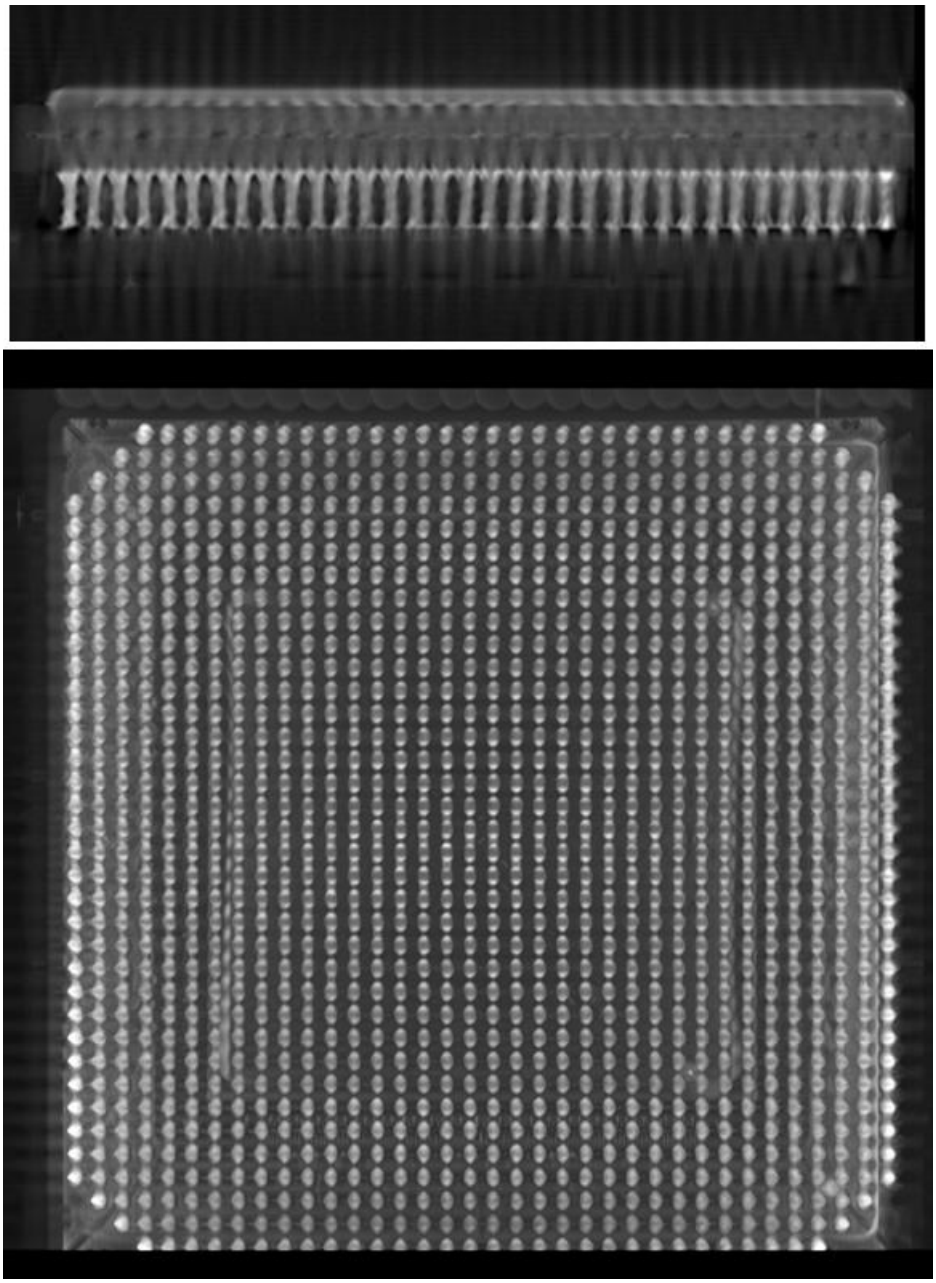

Figure 3.2-8. Slices from 3D X-ray digital data generated by X-section, either vertical or horizontal.

4.0 X-RAY TEST RESULTS FOR 3D STACK ASSEMBLIES

4.1 Optical Inspection of 3D TSOP Stack

A 3D stack package assembly after thermal cycling and failure was selected for both 2D and 3D computed tomography X-ray evaluation to determine if either of the two X-ray systems can detect failures. The 3D package consists of 48 lead TSOPs solder stacked (4-high) and integrated into a single dual-flat no-lead (DFN) packages. Dummy packages were used in a daisy chain configuration for interconnect testing. Pb-free solder was used in the stacking assembly process and 63Sn-37Pb solder was used to mount the package to the test board. An example of the completed assembly is shown in Figure 4.1-1. A number of these assemblies were subject to thermal cycle testing in the range of –55 to +125°C. One failed test sample was selected for failure characterization and comparison by optical microscopy and 2D/3D X-ray systems. The comparison provided key advantages and disadvantage of each inspection system for use in advanced stack electronic packaging.

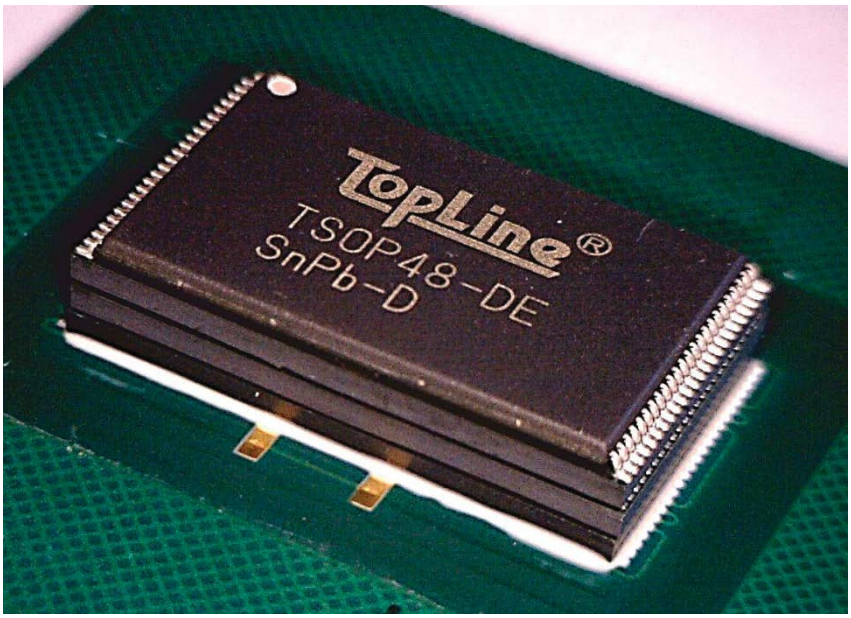

Figure 4.1-1. Photograph of 4-high stacked package surface-mounted assembly with underfill.

Representative optical photographs of a 4-high stack after thermal cycling are shown in Figure 4.1-2. The top photos show an overall feature of the 3D stack package assembly, with some signs of separation of no-lead packages at the center and at the edge. Higher magnification images shown at the bottom clearly show separation and failure due to thermal cycling exposure. The apparent failures are marked with red circles for better identification.

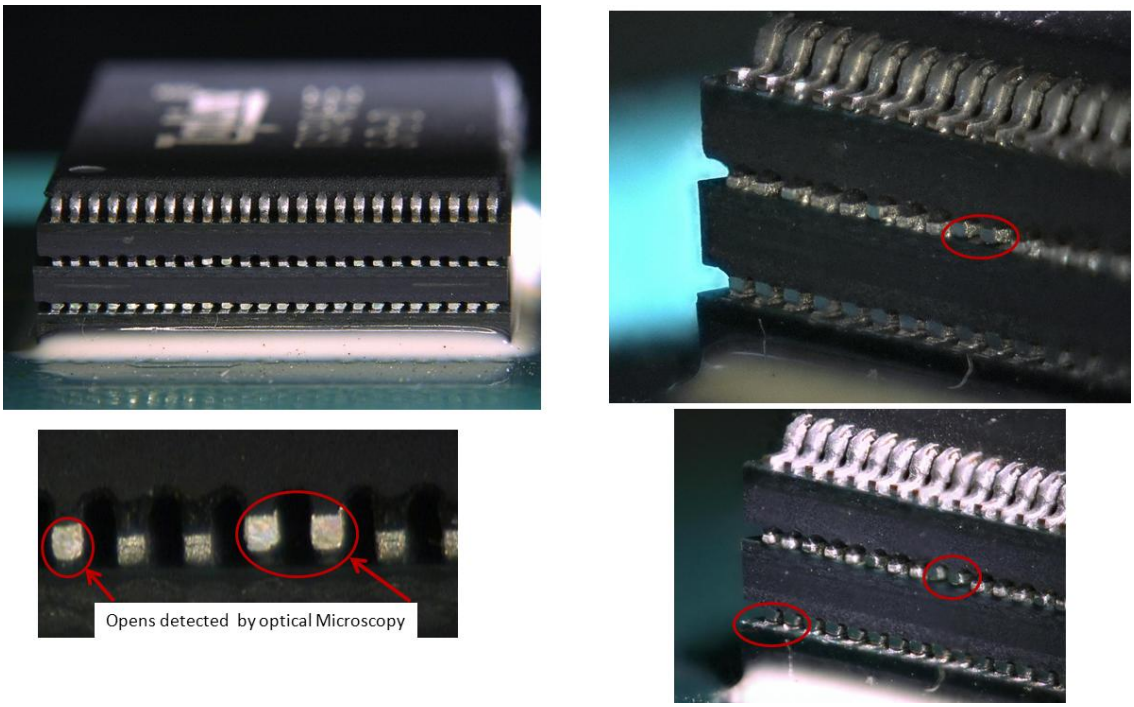

Figure 4.1-2. Photograph of a 4-high stacked package after thermal cycling showing failures of no-leads.

4.2 2D X-Ray of 3D TSOP Stack

Figure 4.2-1 shows a few representative 2D X-ray images for the 4-high TSOP stacked-surface mounted package assembly. These 2D X-ray images were taken at various angles, and other attempts were made to delineate the no-lead failure separations that were clearly apparent from both optical microscopy inspection and images. The result was no clear identification of separation. As apparent from the X-ray images, combining stack leads and copper mesh used in the board made it difficult to distinguish the failure separation, which was easily noticeable via optical microscopy. This is one of the drawbacks of X-ray system; it exposes everything between source and detector.

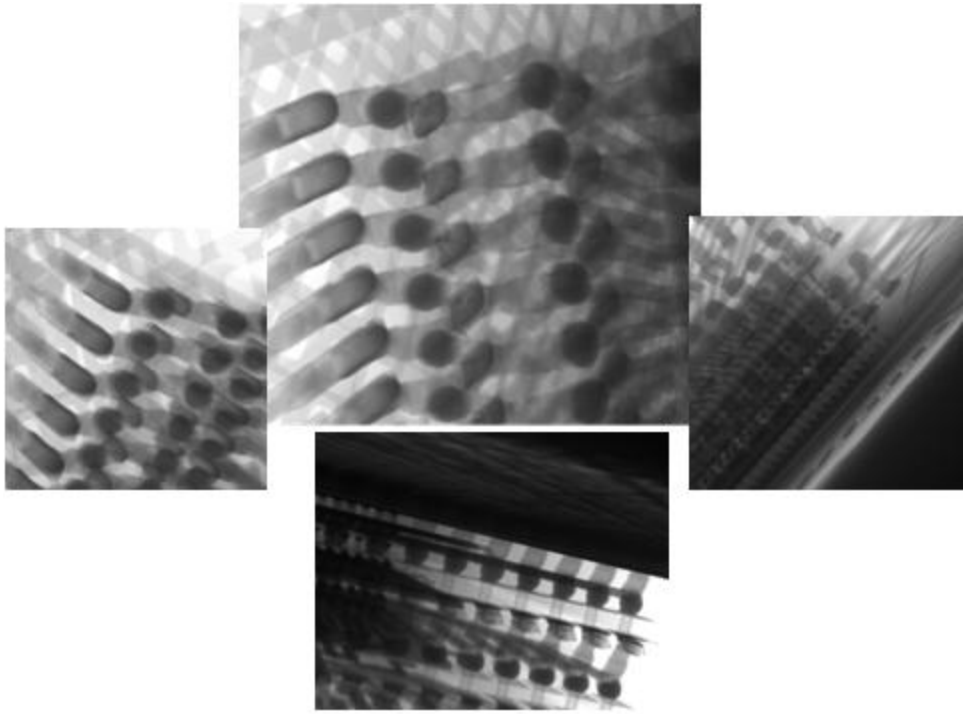

Figure 4.2-1. 2D X-ray images of a 4-high stacked package after thermal cycling in an attempt to delineate failure observed by optical microscopy.

4.3 3D CT X-Ray of 3D TSOP Stack

The X-ray system with the 2D into 3D image transformation was used to characterize thermal cycling damage to a 4-high stacked package assembly. The CT images are automatically created by designing a sample holder for insertion in the rotational motor tool installed in the 2D X-ray. The board assembly was slightly higher than the 3D stack package; therefore, maximum ideal magnification could not be achieved. Figure 4.3-1 shows a representative setup in preparation for generating 3D X-ray images of 3D stack assembly. Rotating the sample allows capturing a series of X-ray images with relative positional coordinates of each image that is captured. These data are stored while the object is rotated within the X-ray beam. When all digital data have been captured, the data bank is processed to reconstruct the cross-sectional 2D or 3D images.

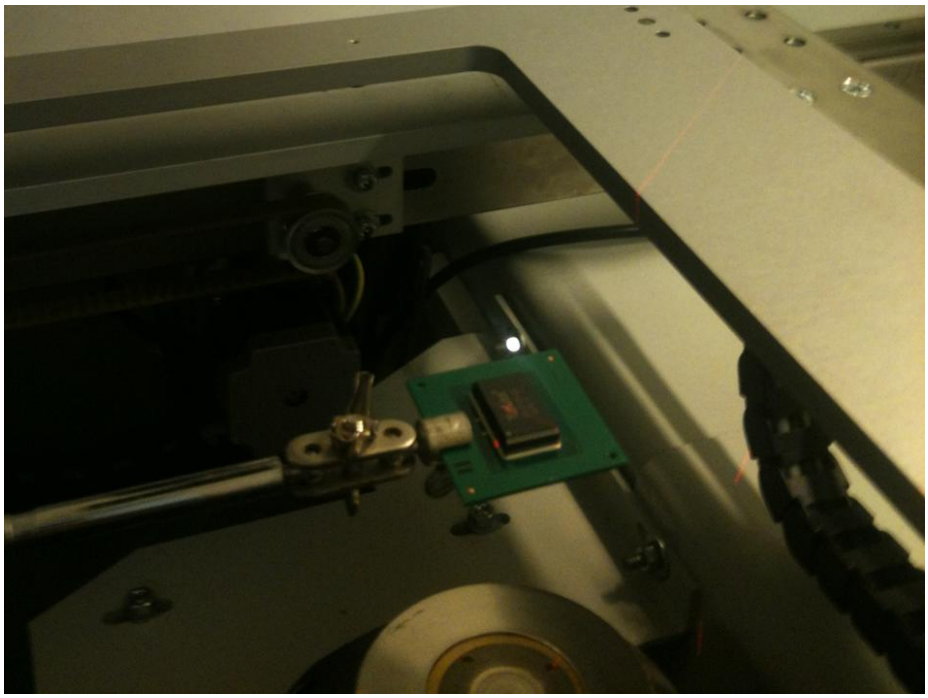

Figure 4.3-1. Photograph of 4-high stack assembly in position and ready for rotation, to generate 3D X-ray images.

Figure 4.3-2 shows an overall 3D X-ray image constructed from the 2D layers. Figure 4.3-3 shows a number of representative x-sectional X-ray images of the same package. Many geometrical features of the 3D stack package are apparent, but resolution is not high enough to distinguish the separation of no-lead solder attachment observed during microscopic evaluation. Even additional attempts to change coloring and better separate various stack layers (see Figure 4.3-4) did not reveal failures that were apparent optically. Low magnification did not allow better identification of damage due to thermal cycling.

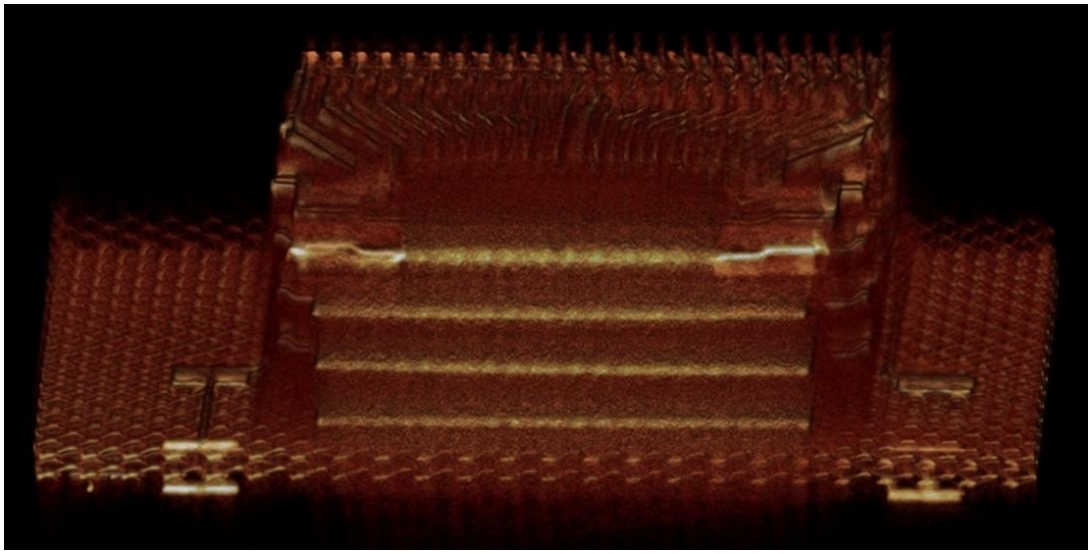

Figure 4.3-2. 3D X-ray images of a 4-high stacked package after thermal cycling showing overall assembly configuration.

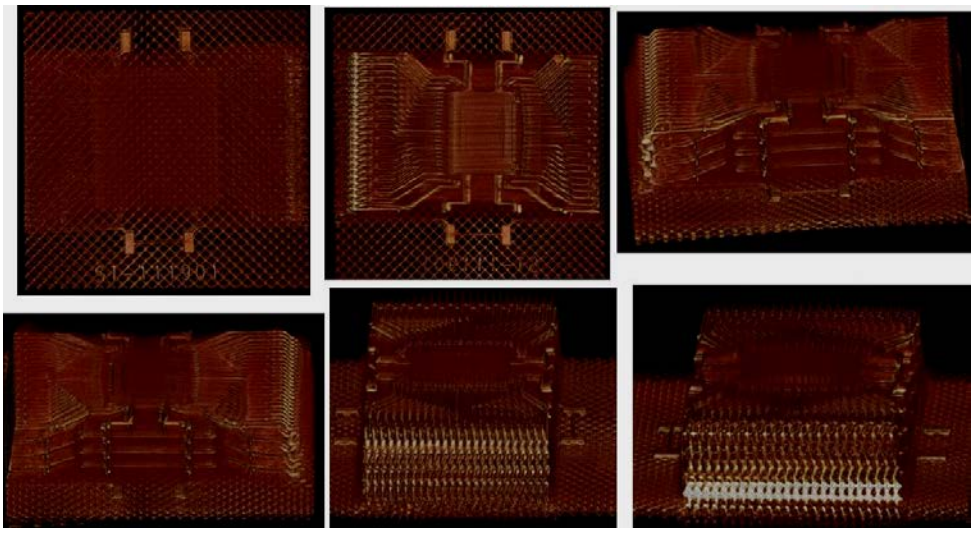

Figure 4.3-3. 3D X-ray slice images of a 4-high stacked package after thermal cycling showing diversity of images that can be generated from the image data set.

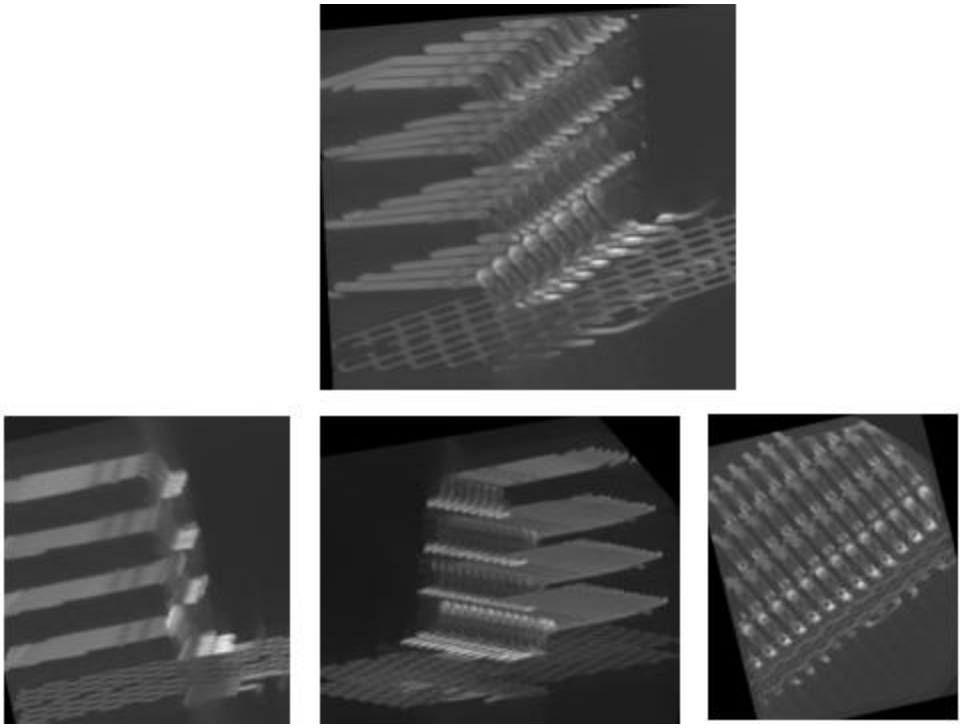

Figure 4.3-4. 3D X-ray slice images of a 4-high stacked package after thermal cycling showing diversity of images, but apparent separation observed by optical microscopy.

5.0 CONCLUSIONS

The evaluations covered in this report deal with inspection methods and comparison of inspection results performed for advanced column grid array and 3D stack package assemblies. Visual inspection using optical microscopy has been the traditional approach for acceptance/rejection of workmanship defects by quality assurance personnel. Inspection of hidden elements in CGA/3D stack assemblies requires using 2D/3D X-ray inspection tools. Two-dimensional microfocus X-ray inspection with a tilt detector capability was used for determination of hidden solder joints and to address damage due to thermal cycling.

With advances in electronic packaging technology, a significant move from 2D to 3D X-ray inspection has occurred to meet the need for miniaturization and expansion in the third dimension. Evaluation of the inspection techniques, optical and 2D/3D systems, revealed the following results.

- Visual inspection using an optical microscope is ideal for detection of solder joint defects such as dewetting, microcracks, cold solder, and disturb solder joints.
- Visual inspection of CGA and 3D TSOP stack package assemblies subjected to a number of thermal cyclings clearly identified solder joint damage, microcracks, and separation.
- Two-dimensional X-ray inspection revealed voids and damage for peripheral columns of CGA assemblies after thermal cycling. However, it was unable to detect microcracks. For the inner columns, even detecting the existence of voids and damage become difficult due to lack of X-ray penetration.
- Two-dimensional X-ray inspection was unable to detect obvious lead separation optically observed for 3D stack assemblies after thermal cycling. Interference from stacked layers and PCB with X-rays was one reason for lack of clear detectability
- Three-dimensional X-ray inspection of CGA revealed only gross tilt of columns due to thermal cycling, but was unable to reveal solder joint damage because of its lower magnification.
- Three-dimensional X-ray images of CGA with Cu spiral columns revealed significantly lower column shift/tilt due to thermal cycling exposure compared to solid solder column CGA.
- Three-dimensional X-ray inspection of a 3D stack package assembly provided configuration of the stacks, but details of solder joint damage (especially gross separation of leads from the pad observed visually) was not revealed.

Given NASA's emphasis on inspection and workmanship, detecting defects on microelectronic packages and assemblies, and understanding key features of various inspection systems in detecting defects in the early stages of assembly, are critical to developing approaches that will minimize future failures. Additional specific, tailored, non-destructive inspection approaches could enable low-risk insertion of these advanced electronic packages.

Even though 2D and 3D inspection by X-ray showed limited defect detection, X-ray inspection is a non-destructive technique with wider use for revealing hidden defects, including solder joints. It is recommended as a complement to other inspection techniques, including traditional visual inspection by optical microscopy. Therefore, a combination of various inspection techniques may be required to be performed in order to assure quality at part, package, and system levels. This is especially true for newly introduced miniaturized advanced electronic packages with hidden solder joints, either as a single or stack entity.

6.0 REFERENCES

[1] Ghaffarian, R. "Thermal Cycle and Vibration/Drop Reliability of Area Array Package Assemblies," *Structural Dynamics of Electronics and Photonic Systems*, eds. E. Suhir, E. Connally, and D. Steinberg, Chapter 22, John Wiley, New York, NY, 2011.

[2] Ghaffarian, R., "Thermal Cycle Reliability and Failure Mechanisms of CCGA and PBGA Assemblies with and without Corner Staking," *IEEE Transactions on Components and Packaging Technologies*, Vol. 31, Issue 2, 2008.

[3] Ghaffarian, R., "Area Array Technology for High Reliability Applications," *Micro-and Opto-Electronic Materials and Structures: Physics, Mechanics, Design, Reliability, Packaging*, ed. E. Suhir, Chapter 16, Springer, New York, NY, 2006.

[4] Ghaffarian, R. "CCGA Packages for Space Applications," *Microelectronics Reliability* **46** 2006–2024, 2006.

[5] Ghaffarian, R., "BGA Assembly Reliability," *Area Array Packaging Handbook*, ed. K. Gilleo, Chapter 20, McGraw-Hill, 2004.

[6] Fjelstad, J., Ghaffarian, R., and Kim, Y.G., *Chip Scale Packaging for Modern Electronics*, Electrochemical Publications, 2002.

[7] Ghaffarian, R., "The Interplay of Surface Mount Solder Joint Quality and Reliability of Low Volume SMAs," *NEPCON WEST Proceeding*, Anaheim, CA, Feb. 25–29, 1996.

[8] Ghaffarian, R., "Solder-Joint Quality with Low-Volume PCB Processing," *SMT Magazine*, July 1996.

[9] Lechner, A., Steffen, J. P., Rother, T., "Microfocus Computed Tomography Extends from the Lab to the Production Floor," Yxlon, 2008.

7.0 ACRONYMS AND ABBREVIATIONS

2D	two-dimension
3D	three-dimension
BGA	ball grid array
CBGA	ceramic ball grid array
CCGA	ceramic column grid array
CGA	column grid array
COTS	commercial-off-the-shelf
CQFP	ceramic quad flat pack
CT	computer tomography
CTE	coefficient of thermal expansion
Cu	copper
FPGA	field programmable gate array
I/O	input/output
JPL	Jet Propulsion Laboratory
LGA	land grid array
MIP	mandatory inspection point
NASA	National Aeronautics and Space Administration
NEPP	NASA Electronic Parts and Packaging
PBGA	plastic ball grid array
PCB	printed circuit board
PWB	printed wiring board
QA	quality assurance
QFP	quad flat pack
ROHS	restriction on hazardous substances
SEM	scanning electron microscopy
SMT	surface mount
TC	thermal cycle
X-section	cross-section